Influence of the primary stress state on the displacement characteristic

C. Leber, N. Radončić & W. Schubert
Institute for Rock Mechanics and Tunnelling,

Graz University of Technology,

Graz, Austria

ABSTRACT: The in-situ stress situation is much more complex than assumed during usual underground excavation design. Even when utilizing more sophisticated, three-dimensional numerical models it is general practice to assume parallel alignment of one of the stress tensor's primary stress components and vertical orientation of one of the other two, hence leading to the usual description of the stress conditions with the K_0 value. These assumptions are somewhat conflicting with current knowledge and assumptions about the influence of the terrain and tectonic regime on the primary stress state. This paper represents the summary of a parametric study, based on results of numerical calculations conducted under assumption of a primary stress state featuring both arbitrary magnitudes of principal stresses and arbitrary spatial orientations. The patterns found in the relationship between displacement behaviour of the tunnel cross section and the primary stress orientations are presented in this paper.

1 INTRODUCTION

For a safe tunnel design it is necessary to take all geotechnical circumstances as groundwater level, geological conditions or primary stress state into account. Regarding the usual implementation of the primary stress state with a K_0 value, it is obvious that for cases with complex initial stress situation this represents a simplification with hardly foreseeable consequences.

Aim of work presented in this paper is an investigation of the interaction of arbitrarily oriented primary stress states with different magnitude with the displacement field caused by the tunnel advance. The results should act as an initial step towards better handling of primary stress state information in the early design stages. In addition, conclusions regarding the primary stress state based on absolute displacement monitoring data have been made possible as well.

A parametric study in FLAC[3D] (2006) has been performed where arbitrarily orientated three dimensional primary stress tensors are implemented by means of the three Euler angles (Mase 1970), which allow an easy mathematical description of the orientation of the stress tripod in space. The calculations feature a systematic variation of the ground characteristics and of the magnitudes of primary stresses.

2 EVALUATION METHODS

2.1 *General considerations*

The ability to easily compare displacement fields of different orientations had top priority, in order to find patterns allowing prediction of displacements by simple calculations in the planning period. The basis has been laid by FLAC[3D] (2006) calculations of a tunnel advance in an arbitrarily oriented primary stress situation. The displacement field is written in global x, y and z directions of grid points in one cross section for each excavation step. In order to cope with such amounts of information, simple methods have been developed and implemented, providing simple, graphic illustration and interpretation. The basis primary stress state used and described in this chapter forms the situation shown in the spherical projection (Fig. 1).
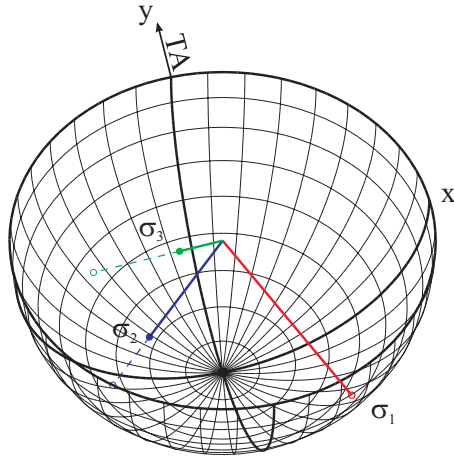
Figure 1. Primary stress situation discussed in this chapter.

2.2 Illustration of three dimensional displacements

The first step in assessing the resulting displacement field is the display of the three dimensional displacement paths of each point in the cross section. The position of the face is marked as a black point. For easier interpretation, projections on horizontal and vertical planes parallel to the tunnel alignment have been added.
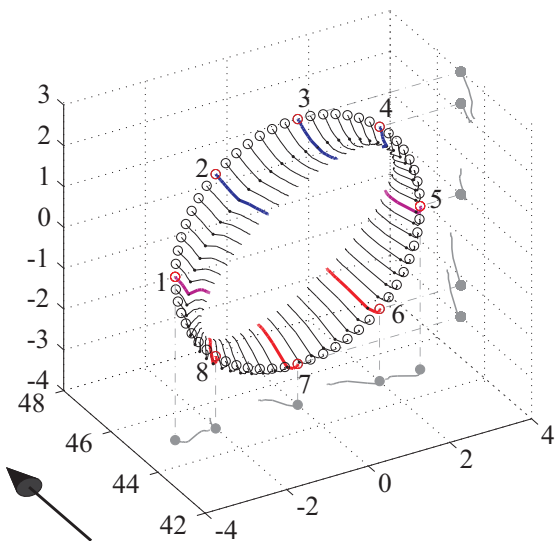

Figure 2. Three dimensional displacement characteristic containing pre-displacements.

2.3 Vectors of displacements in spherical projection

An easy comparison of different cases and indication of the trend of deformation is given by plotting the displacement vector orientations of chosen points along the reference cross section in the spherical projection. Connecting the points where the vectors intersect the surface of the hemisphere makes it possible to evaluate the results and find similarities in different cases.

When interpreting the spherical projection plot particular attention should be paid to the fact that vectors are not projected into one hemisphere as usually applied, but into a complete sphere shown in horizontal projection. Colors allow differing between upper and lower hemisphere: Points intersecting the lower hemisphere are shown in black while the ones intersecting the upper hemisphere are shown in grey.
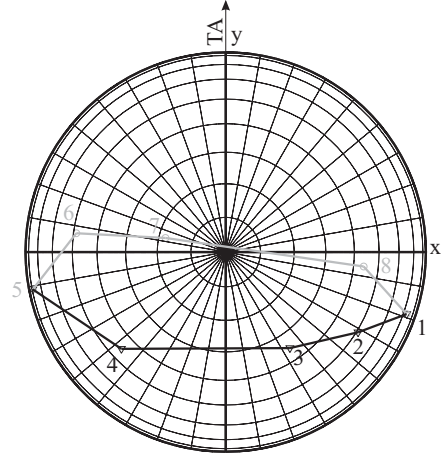

Figure 3. Displacement vector view in spherical projection.

When observing deformation of the lower right bench (point 6) in Figure 3, a trend into advance direction and left upwards can be distinguished, being observable in Figure 2 as well.

The method shown in Figure 3 has the drawback of omitting the deformation magnitudes.

2.4 Normal vectors of the deformed cross section

A simple method for the analysis of spatial displacement behavior during tunnel advance has been developed as well, given by calculating the normal vector of the best-fit plane to the deformed cross section. The fitting of the plane is realized by finding the minimum of the normal distances between points in momentary configuration and the plane defined by its origin point (in the respective cross section) and a normal vector. The calculation of the respective best-fit normal vector is performed after every advance step. Drawing the points where the normal vectors intersect the unit sphere in the spherical projection leads to identification of a deformation trend of the entire cross section. In order to correlate this trend to the primary stress state, the tripod spanned by the principal stresses of the primary stress tensor is also shown in the Figure 4.

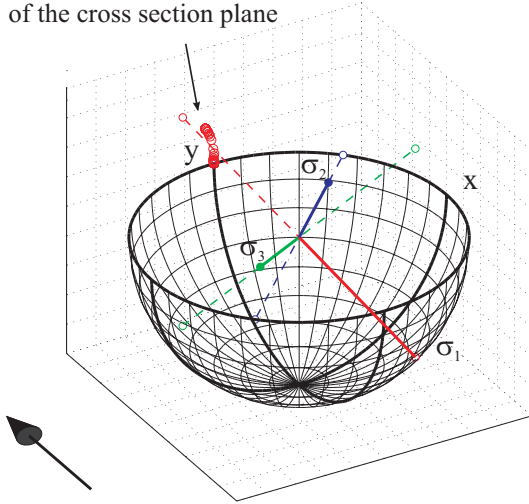Intersection of normal vectors
of the cross section plane

Figure 4. Development of normal vectors of cross section for each excavation step.

The determination of the general pattern in the relationship between primary stress tensor and the displacement field has been performed by calculating the spatial angle spanned by the normal vector and the principal stress vectors of the primary stress state by using the scalar product (hence determining the cosine between them). If the calculation is performed for every excavation round and plotted in a diagram, an easy comparison and interpretation of the spatial displacement characteristic is possible.

2.5 *Interpretation of radial displacements*

There is a number of studies with regard to the relationship between development of radial displacement, tunnel advance and depth of the failure zone. The work of Panet and Guenot (1982) represents an almost perfectly fitting empirical relation between depth of failure zone, relative distance to the tunnel face and radial displacement process (assuming hydrostatic primary stress state). The ability of this relationship to predict the displacement development in cases of an arbitrary primary stress state has been put to scrutiny as well, and yielded favorable results.

2.5.1 *Radial displacement development*
Panet and Guenot (1982) generate an essential equation for tunneling, describing the displacement path against the distance to the face at one point of the tunnel intrados. Input parameters are the final displacements assuming infinite distance between observed point and the heading face and the plastic radius (both usually obtained by a plane strain closed-form solution). The equation writes as:

$$C(x) = C_f + \left(C_\infty - C_f\right)\cdot\left[1 - \left(\frac{0{,}84\cdot r_p}{0{,}84\cdot r_p + x}\right)^2\right] \tag{1}$$

where $C(x)$ = radial displacements in relation to the face distance x; C_f = value of predisplacements, C_∞ = final radial displacements, and r_p = plastic radius.

The calculation of the radial pre-displacements is performed by using the equation of Hoek & Caranza-Torres (2008), the calculation of the plastic radius using equations of Feder & Arwanitakis (1976).

Normalizing the radial displacement output of numerical calculations allows their comparison to radial displacements using equation of Panet & Guenot (1982). Different radial displacement paths for different points along the tunnel intrados are observed, which is a consequence of the non - hydrostatical primary stress state (forming a nearly elliptical plastic zone).

2.5.2 *Radial displacement versus radially directed primary stress tensor components*
For an arbitrarily oriented primary stress state multiplying the tensor by Equation (2) calculates that part of stress tensor that shows into radial direction. A unit vector implemented in the cross section plane and pointing outwards defines the radial direction. The respective normal component of the Cauchy stress is obtained by multiplying the primary stress tensor twice with the radial unit vector.

$$\sigma_r = [P]\cdot(R)\cdot(R)^T \tag{2}$$

where σ_r = radial part of primary stress tensor; [P] = primary stress tensor and (R) = radial unit vector.

Due to the symmetry of the primary stress tensor, there are always double minima and maxima of the radial stress component, forming two axes of minimal and maximal radial stress, respectively.

A three dimensional diagram of radial displacements against excavation steps and angle around tunnel perimeter (counterclockwise positive) serves as visualization of the relationship between the excavation process, associated stress re-distribution and displacement development.

3 RESULTS OF PARAMETER STUDY

3.1 *Cases studied*

In order to find re-occurring patterns that enable prediction of displacement behavior, 22 different orientations of primary stress state are analyzed by rotating the stress tripod in steps of 45°. In addition, varying strength parameters and constitutive models (elastic, Mohr-Coulomb) for each orientation yield to three different depths of failure zone:
- linearly elastic model
- elastic or slightly plastic: Mohr-Coulomb plasticity with strength parameters set to such values that no plastic zone occurs in a hydrostatic stress state, however when rotat-

ing and adding deviatoric components a slight and localized plastification occurs.
- plastic: Mohr-Coulomb plasticity with strength parameters set to have a depth of plastic zone of 3 m in the hydrostatic component of the primary stress state.

The influence of volume increase when at yield has been checked as well by activating dilatancy in special, chosen cases. All in all, 77 different cases have been analyzed and form the base for the search for patterns, using the interpretation methods described above.

3.2 Rotation of cross section plane

The normal vector of each cross section plane, spanned by the current measuring points, always rotates in direction of the highest principal stress of the primary stress state, when having a spatially inclined primary stress orientation. This phenomenon emerges in all cases, independent of the proportions of principal stresses (in primary stress state) and material parameters. The principal stress proportions and material parameters and/or their interaction just affect the magnitude of cross-section rotation and the development when advancing the tunnel; the trend itself always stays the same. Comparing the diagrams of spatial angles spanned by the normal vector and the three mean normal stresses shows a decrease of the spatial angle "development rate" with increasing depth of failure zone.
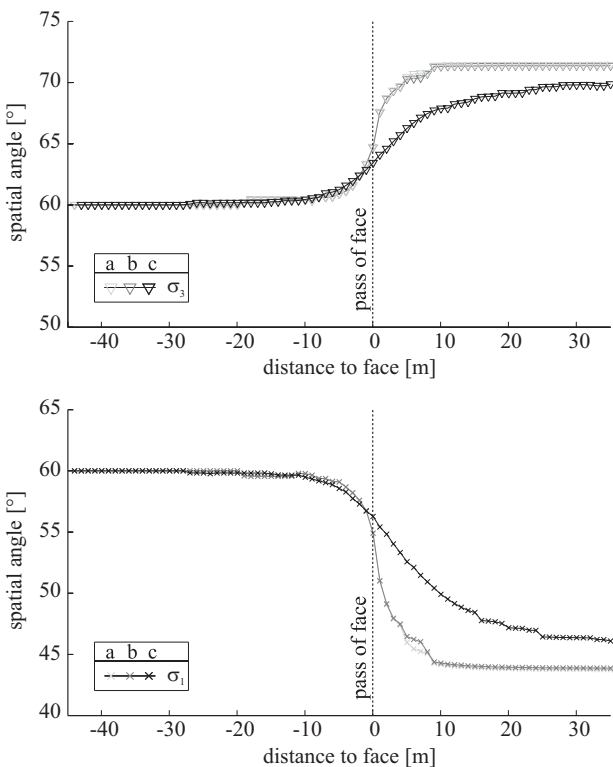

Figure 5. Comparison of spatial angles spanned by normal vector of cross section plane and smallest primary mean normal stress σ_3 (above), highest primary mean normal stress σ_1 (below) while excavating.

Figure 5 compares the three cases linearly elastic (a), slightly plastic (b) and plastic (c) for the reference orientation (Fig. 1) and principal stresses of 10, 15 and 5 MPa.

It has to be remarked that the displacements are magnified for visualizing the change of the spatial angle. The magnitude of the original angle would be approximately 1°.

3.3 Radial displacements

The deeper the failure zone is, the smaller is the difference between minimal and maximal radial displacements. The mechanism of rearrangement of stresses when having deep failure of the ground causes a general, almost concentric convergence. The surface that can be seen when looking at radial displacements at the unrolled cross section flattens with the increasing depth of the plastic zone. The comparison between a slightly plastic and plastic case of the reference orientation (Fig. 1) is shown here.
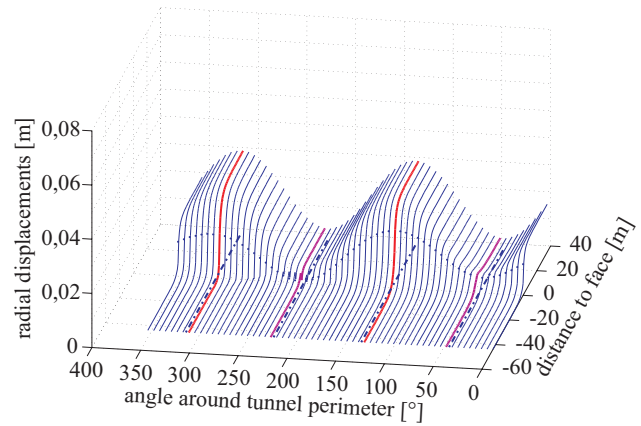

Figure 6. Radial displacement across tunnel excavation and along the unwound cross section of slightly plastic case.
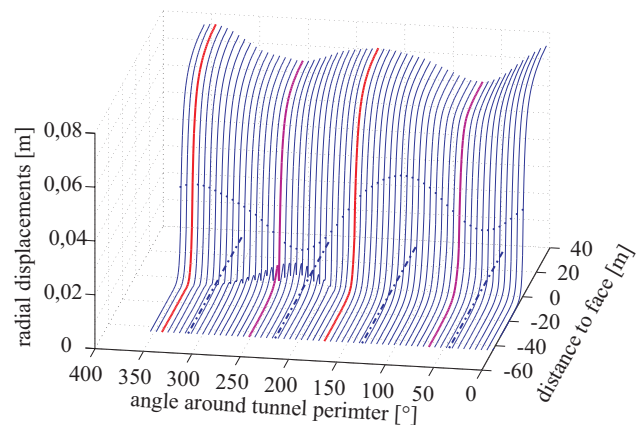

Figure 7. Radial displacement across tunnel excavation and along the unwound cross section of plastic case.

On the base of the diagrams in Figure 6 and 7 the position (dot and dash line) of minimal and maximal radial components of primary stresses is shown. The face passage is marked with a point.

The minimal and maximal radial displacements correspond with minimal and maximal radial parts of primary stresses for slightly plastic cases. In plastic cases this can be observed as well, except in cases where maximum and middle principal stress point into tunnel direction and the stress tensor is generally consideably rotated with respect to the tunnel axis.

Needless to say, the orientations with constant radial normal stress components also yield constant radial displacement fields.

3.4 *Comparison of radial displacements to relationship by Panet and Guenot (1982)*

The normalized radial displacement development of all points around tunnel perimeter correlates well with the displacement path as obtained by relationship of (Eq. 1), if the final convergence is replaced by "1". .
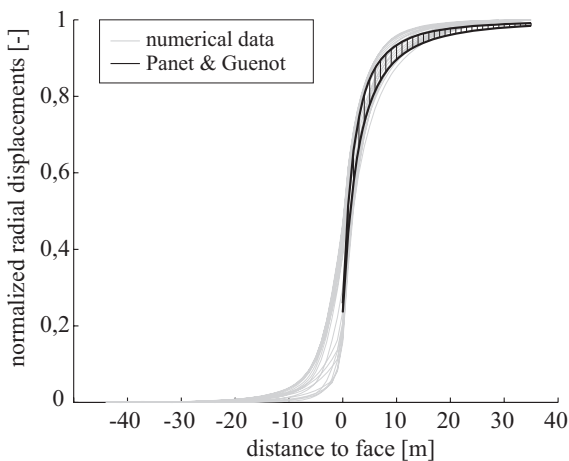
Figure 8. Normalized radial deformation compared to normalized displacement development after Panet & Guenot (1982).

The input parameter plastic radius for development after Panet & Guenot (1982) induces different results for different points along tunnel perimeter (non-hydrostatic stress state as mentioned in 2.5.1), thus resulting in a range of displacement paths (black area). Numerical simulations also yield a range of displacement paths (grey curves).

Therefore the relation, that defines the development of radial deformation as just dependent on depth of failure zone, holds good also for rotated primary stress situations.

Generally must be noted that anisotropy of rock mass properties has big influence on displacement characteristics (on magnitudes as well as on development). Hence the statement above just holds true when the failure mechanism stays the same. Cases where failure mechanisms are caused by development of distinct shear bands or problems with stability (buckling failure) are excluded from this work.

4 CASE STUDY: GALGENBERG FAULT ZONE

Reasons for a rotated primary stress orientation can all be generally derived from the geological and topographical situation (overconsolidation, tectonic processes, vicinity of a slope et cetera).

A particular situation was encountered when tunneling through the "Hinterberg" fault in the Austrian "Galgenberg"-tunnel.
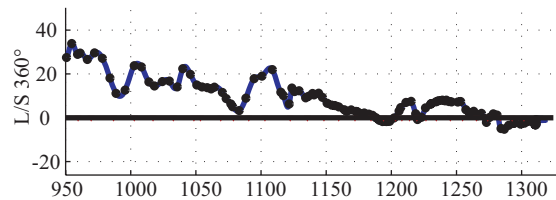
Figure 9. Trend line of the vector orientation (L/S) on the crown 15m behind the face.

Figure 9 represents the trend line of the vector orientation (L/S) on the crown 15 meters behind the face. The vector orientation trend (L/S) decreases from an unusually high value (displacement vector tends more against the direction of excavation) at the beginning of the fault zone to a relatively low value (meaning displacements parallel to the plane of the respective cross-section) when approaching the end of the fault area. This general trend was believed to be caused by specific primary stress conditions.
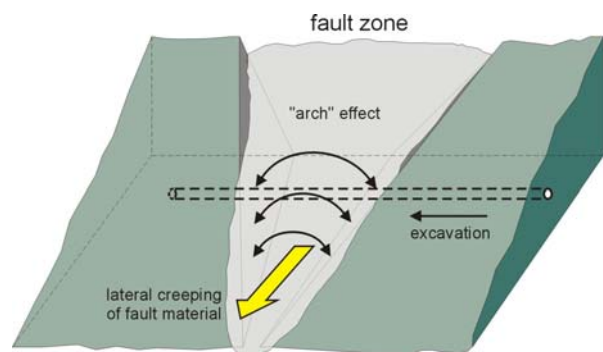
Figure 10. "Hinterberg" fault zone wedged between two massive block bodies (Schubert & Riedmüller 1995).

Considering the geological and topographical situation in this area, the assumption of a rotated primary stress state appears to be plausible. Stress trajectories in the fault material wedged between two massive dolomite bodies form an arch as a result of a lateral creep process of the fault material and competent dolomite acting as an abutment. When entering the fault the highest principal stress shows diagonally from top right to left down. When passing the fault it is exactly the opposite.

To proof this assumption, numerical simulations with similar stress conditions (highest primary stress

vector dips 45° against direction of excavation when entering, and 45° in direction of excavation when leaving the fault zone - lateral influence disregarded) have been conducted and the results have been investigated.
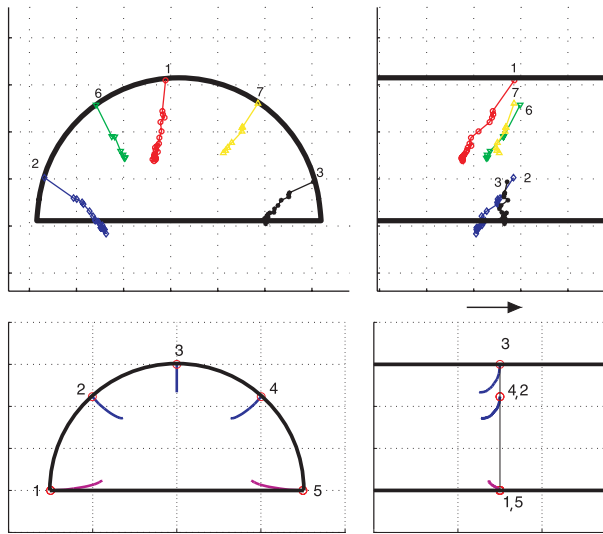

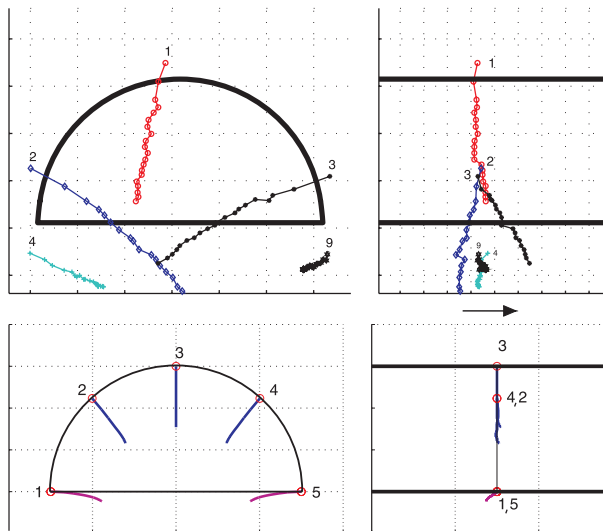Figure 11. Entering the fault zone: measured data (above) compared to numerical data (below).

Figure 12. leaving the fault zone: measured data (above) compared to numerical data (below).

The measured data correlates well with numerical data. (The variations of right sidewall when leaving the fault are caused by disregarded lateral influence of primary stress state in the numerical simulations) When comparing the diagrams of Figures 11 and 12 with the trend line of the crown displacement vector orientation (Fig. 9) the same trend can be observed.

5 CONCLUSION

With the interpretation methods devised for this work it has been possible to show a clear relationship between the displacement characteristic and the primary stress state. It points out that in some cases the knowledge of the initial stress situation (not only of the stress magnitudes) is essential for an economical and safe tunnel design. Knowing that the normal vector of the cross section plane always rotates into direction of the highest primary stress vector provides a basis for displacement prediction. Further work will be invested into modeling more realistic excavation geometries and support measures, allowing the determination of the influence of the primary stress state on the system behavior in a more accurate, realistic model. In addition, the issue of interaction between geological structure and primary stress state, leading to different modes and magnitudes of structurally driven failure, is currently left largely untreated.

REFERENCES

Feder, G. & Arwanitakis, M. 1976. Zur Gebirgsmechanik ausbruchsnaher Bereiche tiefliegender Hohlraumbauten (unter zentralsymmetrischer Belastung), Berg- und Hüttenmännische Monatshefte, Jahrgang 121, Heft 4.

Hoek, E.,Carranza-Torres, C., Diederichs, M.S. & Corkum, B. 2008. Integration of geotechnical and structural design in tunnelling, Proceedings University of Minnesota 56th Annual Geotechnical Engineering Conference. Minneapolis, 29 February 2008, 1-53

Itasca Consulting Group, Inc. 2005. FLAC[3D] Fast Lagrangian Analysis of Continua in 3 Dimensions User's Manual. 2nd Edition. Minesota.

Mase G., 1970. Theory and Problems of Continuum Mechanics, Schaum's Outline Series, McGraw-Hill, USA

Panet, M. & Guenot, A. 1982. Analysis of convergence behind the face of a tunnel, Tunnelling 1982, The Institution of Mining and Metallurgy, S. 197-204.

Schubert, W. & Riedmüller, G. 1995. Geotechnische Nachlese eines Verbruches – Erkenntnisse und Impulse. Mitteilungsheft des Institutes für Bodenmechanik und Grundbau TU-Graz. Heft 13, S. 59-68.